ACS Catalysis

Research Article

pubs.acs.org/acscatalysis

Common Pathways in Ethanolysis of Kraft Lignin to Platform Chemicals over Molybdenum-Based Catalysts

Xiaolei Ma,[†] Rui Ma,[†] Wenyue Hao, Mengmeng Chen, Fei Yan, Kai Cui, Ye Tian, and Yongdan Li*

Collaborative Innovation Center of Chemical Science and Engineering, Tianjin Key Laboratory of Applied Catalysis Science and Technology, State Key Laboratory of Chemical Engineering, School of Chemical Engineering, Tianjin University, Tianjin 300072 People's Republic of China

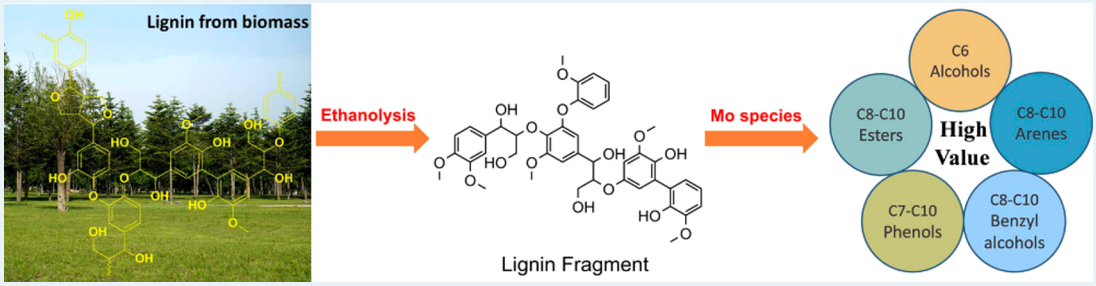

ABSTRACT: One-pot complete catalytic ethanolysis of Kraft lignin into C6−C10 chemicals, that is, aliphatic alcohols, esters, phenols, benzyl alcohols, and arenes, is achieved with a batch reactor over a number of supported molybdenum-based catalysts at 553 K in pure ethanol under autogenous pressure of 10.6 MPa. Metallic molybdenum, its carbide, and nitride all show remarkable activity, with the carbide and metallic catalysts giving the higher overall yields: 1640 and 1390 mg/g lignin, respectively. The major phases composing the catalysts are well-preserved after the reaction; however, the detection of Mo(V) species verifies the partial oxidation of molybdenum, which leads to the formation of the dissociative Mo species, such as molybdenum V ethoxide, in the fluid phase. Through the product analysis and catalyst characterization, the common route of lignin conversion to value added chemicals over the Mo-based catalyst is presented in detail. Kraft lignin is first fragmented into segments with $m/z \sim 700-1400$ via a noncatalytic ethanolysis process. Meanwhile, the main active Mo(V) species dissociate from the solid catalyst into the fluid due to the interaction of ethanol. Then mainly the dissociative species catalyze, with the participation of the radicals, the further degradation of the segments into small molecules.

KEYWORDS: *lignin, depolymerization, heterogeneous catalysis, chemicals, molybdenum, supercritical ethanol*

1. INTRODUCTION

The diminishing reserves and the increasing consumption of fossil fuels necessitate the development of fuel and chemical production routes from alternative resources.[1−3] As early as the 1940s, experimental data from Berl[4] supported the concept of hydrocarbon oil production from biomass. Recently, Regauskas et al.[5] outlined the spectrum of lignin valorization research activities, ranging from genetic engineering approaches to chemical processing techniques. Lignin, the second most abundant natural polymer, just after cellulose, and the least utilized biomass fraction, is a complex and irregular macromolecule constituted mainly of hydroxyphenyl propanes and aliphatic chains.[6−8] Kraft lignin refers to the byproduct of the largest biomass utilization process, that is, the Kraft wood-pulp and straw milling processes for separating cellulose from lignocellulosic biomass to make paper. Kraft lignin had been an important pollution waste and has been isolated from the black liquor in recent decades as a low-heating-value fuel for recovering the energy and alkaline metal salts. However, Kraft lignin is not a good fuel, with lower heating value and higher poisonous gas emissions than the case with coal used as a boiler fuel. In recent years, because of the development of cellulose utilization processes as energy feedstocks (e.g., bioethanol), the amount of available isolated lignin increased substantially. The worldwide Kraft lignin production from the pulp and paper manufacturers has exceeded 50 million metric tons annually.[9] Because of the diversity of its monomers and its markedly lower oxygen content than that of polysaccharides, lignin is a promising feedstock for the production of renewable replacements of petroleum-derived products.[6,7,9−15]

Yan et al.[16] investigated the selective degradation of wood lignin over a number of noble metal catalysts via a two-step process in near-critical water with an initial 4 MPa of H_2. Their process yields about 42 wt % C8−C9 alkanes, 10 wt % C14−C18 alkanes, and 11 wt % methanol. For the production of monomeric aromatic compounds from lignin, noble metal catalyst and conventional hydrotreating catalyst were used successively, also through a two-step approach reported by Weckhuysen's group.[14,17] In the process, lignin was first depolymerized in an alkaline ethanol−water (1:1, v/v) mixture

Received: March 14, 2015
Revised: July 5, 2015
Published: July 7, 2015

DOI: 10.1021/acscatal.5b01159
ACS Catal. 2015, 5, 4803−4813

over Pt/Al_2O_3 at 498 K, with a final 5.8 MPa maintained by Ar, and then the obtained lignin oil was subjected to a hydrodeoxygenation (HDO) reaction over conventional hydrotreating $CoMo/Al_2O_3$ and Mo_2C/CNF catalysts in dodecane at 573 K, with a final 5.0 MPa of pressurized H_2. The final products with low oxygen content were obtained, and the yield of monomeric aromatic products was up to 9%. In addition, the authors observed that some of the monomers were ethoxylated, and they pointed out that this will lower their repolymerization tendency.[17]

One-pot conversion of pine wood flour to liquid fuels in supercritical methanol (573−593 K, 16−22 MPa) over a copper-doped porous metal oxide catalyst and under H_2 atmosphere obtained from methanol reforming and water gas shift reactions has been reported.[18] The liquid products from the reaction at 593 K for 8 h contain 9.1 wt % C2−C6 higher alcohols and ethers, and 4.0 wt % C9−C12-substituted cyclohexyl alcohols and ethers. Recently, $CuMgAlO_x$ catalyst was proved to be active for aromatic compound production from Kraft lignin in supercritical ethanol.[19] The authors reported a yield of monomers of 23 wt % without char formation and also detected ethyl esters at 573 K for 8 h under nitrogen atmosphere. With various solid acid catalysts, including zeolites, clay, niobium pentoxide, and MoO_3/SiO_2, and under an initial 0.7 MPa N_2 atmosphere in H_2O-CH_3OH (1:5, v/v) solvent, efficient conversion of different types of lignin into value-added aromatic monomers at 523 K has been reported.[20]

The formation of aromatic monomers with ∼90% selectivity was achieved through analysis of the organic solvent extracted products. With NaOH as a cocatalyst and HZSM-5 or Ni-doped HZSM-5 as the catalyst in H_2O-CH_3OH (1:1, v/v) solvent at 493 K with an initial 0.1 MPa of Ar, lignin was also effectively converted to value-added hydrocarbons without char formation.[21] Ni-based catalysts were proved to be effective in the lignosulfonate conversion under mild conditions, offering a high conversion of >60% and selectivity of 75−95% for alkane-substituted guaiacols, that is, 4-propyl-guaiacol and 4-ethyl-guaiacol, with an initial 5.0 MPa of H_2 at 473 K in ethylene glycol and glycerol.[22]

For the valorization of native birch wood lignin into monomeric phenols in common alcohols such as methanol, ethanol, and isopropyl alcohol, nickel-based catalysts were evaluated at 473 K under an inert Ar atmosphere.[15] At a lignin conversion of about 50%, an overall selectivity of propylguaiacol and propylsyringol of >90% was obtained. The fragmentation−hydrogenolysis mechanism of lignin depolymerization in alcohol over nickel-based catalysts was proposed. Furthermore, confirmed by isotopic tracing experiments, alcohols provide active hydrogen species, whereas the presence of gaseous H_2 has no effect on lignin conversion. Different Mo-based catalysts, containing MoS_2, MoO_2, Mo_2C, and $NiMo/Al_2O_3$ (in oxide, reduced and sulfide form) have been tested to be active in the hydrotreatment of liquefied lignocellulosic biomass in hydrogen donor solvent at 573 K and 8 MPa of final hydrogen pressure.[23−25] Recently, we reported the complete ethanolysis of Kraft lignin under supercritical conditions over an activated-carbon-supported α-molybdenum carbide catalyst, giving a remarkably high yield, 1.64 g/g lignin, of C6−C10 oxygenated and aromatic chemicals without formation of char and tar.[26] These C6−C10 oxygenated and aromatic chemicals are perfect octane number boosters and fine commodity chemicals if separated. Ethanol was found to be the only effective solvent so far for Kraft lignin conversion over the carbide catalyst. However, if pure water, methanol, and isopropyl alcohol were used as the solvents, the yields were remarkably low. The promising result stimulated great interest in the activity of molybdenum in the supercritical ethanol reaction system. Herein, a number of supported molybdenum-based catalysts are examined in supercritical ethanol under the same conditions as our reported work[26] to disclose the common features of the molybdenum catalysts and illuminate the underlying reaction pathways of the lignin conversion reactions.

2. EXPERIMENTAL SECTION

All of the Mo-based catalysts were prepared using an incipient impregnation technique as the first step with Mo loading of 30 wt %, and with $(NH_4)_6Mo_7O_{24}\cdot 4H_2O$ as the precursor. MoO_3/Al_2O_3 was obtained after drying and calcination at 773 K for 4 h in air. The metallic Mo was prepared under H_2 flow, 210 mL/min, at a final temperature of 1023 K for 2 h after drying. The catalyst reduction temperature has been optimized in our study.[27] The nitride was obtained in a N_2/H_2 flowing gas, total of 210 mL/min in 1/5 ratio, at a final temperature of 973 K for 1 h after drying. The carbide was prepared according to a published paper.[26] The lignin used was purchased from Sigma-Aldrich with product number 471003, and the detailed characterization of the lignin was provided in a published paper.[26] The alumina was kindly provided by CNOOC Tianjin Chemical Research & Design Institute. The activated carbon was supplied by Norit Co. Ltd., Netherlands. All the other used solvents and chemicals of analytical grade were purchased from Tianjin Guangfu Technology Development Co. Ltd., China.

The lignin conversion experiments were carried out in a Hastelloy stirred tank reactor (Parr 4560, 300 mL) at 553 K for 6 h, loaded with 1.0 g of lignin, 0.5 g of catalyst, and 100 mL of ethanol. Nitrogen was used to purge the reactor after the reactor was loaded and sealed. The initial pressure of the reactor was 0.1 MPa of nitrogen (absolute pressure). The final reaction pressure at 553 K was around 10.6 MPa and changed in a range (±0.2 MPa) as different catalysts were used. After reaction, the liquid products were obtained by filtration. Product identification was achieved using GC/MS (Agilent 6890-5973) equipped with a NIST 2.0 database. The product yields were calculated with *o*-cresol as the internal standard by GC/FID analysis (Agilent 6890) and denoted as milligrams per gram of lignin. The chromatographic columns used for both the GC/MS and the GC/FID were HP-5MS (30 m × 0.25 mm × 0.25 μm). The oven temperature program was both set from 318 K to a final temperature of 523 at 10 K/min and then held at the final temperature for 2 min. A split ratio of 50 was used, and the injection temperature was set at 573 K.

X-ray diffraction patterns (XRD) were measured with a powder diffractometer (Bruker AXS D8-S4) operated at 40 kV and 40 mA, using a Cu Kα radiation source. The scanning was conducted between 2θ of 20 and 80° with a scanning rate of 8°/min. N_2 physisorption isotherms were recorded with a Quantachrome Autosorb-1 at 77 K. Prior to measurement, the samples were degassed under vacuum at 523 K for 6 h. The surface area was obtained using the BET method at relative pressures (P/P_0) ranging from 0.05 to 0.30. The total pore volume was derived from the adsorption amount at a relative pressure of 0.99.

High-resolution transmission microscopy was carried out on a JEOL-JEM-2100F electron microscope operating at 200 kV.

DOI: 10.1021/acscatal.5b01159
ACS Catal. 2015, 5, 4803−4813

Before observation, the sample was ultrasonically suspended for 30 min and then deposited onto a copper grid coated with a carbon film. Infrared spectra were collected at room temperature on a Fourier transform spectrometer (Nexus, Thermo Nicolet Co.) with a resolution of 4 cm^{-1} for 32 scans in the region 4000−400 cm^{-1}. Pellets were prepared by mixing 10 mg of sample in 150 mg of KBr. Electron paramagnetic resonance (EPR) experiments were performed using Bruker-A300 apparatus at liquid nitrogen temperature, and the sample was loaded into the EPR cell. A microwave frequency of 9.41 GHz, 2 G modulation amplitude, and 160 mW microwave powder were used.

3. RESULTS AND DISCUSSION

3.1. Analysis of Products Obtained over Different Mo-Based Catalysts. In our recent work, it was obvious that ethanol takes part in the reaction and contributes to the formation of the aliphatic molecules and the ethanol esters with the aromatic compounds, thus leading to the overall product's yield exceeding 1000 mg/g lignin.[26] In this work, three new Mo-based catalysts, MoO_3/Al_2O_3, Mo/Al_2O_3, and Mo_2N/Al_2O_3, are examined. The product compositions obtained over the three catalysts are found similar to those obtained with the α-MoC_{1-x}/AC catalyst, mainly consisting of esters, alcohols (i.e., aliphatic alcohols), and aromatics.[26] Here, we quantified 27 (denoted as P27) components in the liquid product and identified another 29 molecules without quantification because of their low content. The yields of the P27 here were calculated with a same method as reported.[26] The qualified molecules are less than or the same as those of the 52 in the published work.[26] Figure 1 gives a comparison of the yields of the P27 in three

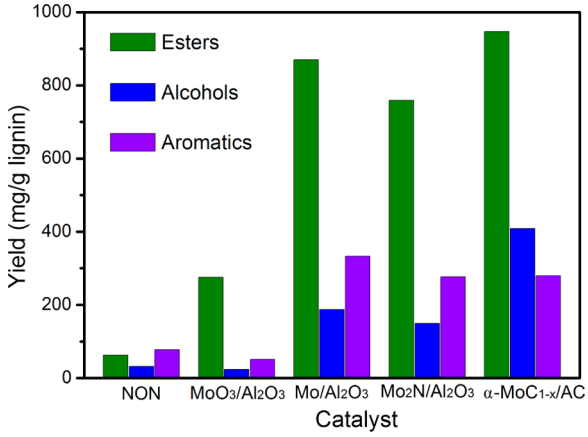

Figure 1. Grouped product yields obtained from lignin valorization over different Mo-based catalysts. (Reaction conditions: 1.0 g of alkaline lignin, 0.5 g of catalyst, initial 0.1 MPa of N_2, 100 mL of ethanol, 553 K, 6 h; "NON" means no catalyst was used.)

groups with and without a catalyst. Without a catalyst, the reaction proceeds, but the overall P27 yield is only 173 mg/g lignin, in which 78 mg/g lignin is contributed by aromatic compounds. The overall P27 yields are 220 and 170 mg/g lignin, respectively, with just AC and Al_2O_3 supports added. However, with the molybdenum catalysts involved, the yield as well as the product distribution changed greatly. For the Mo catalyst in an oxide state, MoO_3/Al_2O_3, the overall yield of the P27 is 351 mg/g lignin. The highest total P27 yield is up to 1640 mg/g lignin over the α-MoC_{1-x}/AC catalyst. The yield values are 1390 and 1185 over the Mo/Al_2O_3 and Mo_2N/Al_2O_3 catalysts, respectively. Among the diverse products, esters account for the most, ranging from 58 to 79 wt % for the respective catalysts. Over the MoO_3/Al_2O_3, Mo/Al_2O_3, and Mo_2N/Al_2O_3 catalysts, the second highest grouped product is aromatics, whereas over the α-MoC_{1-x}/AC catalyst, the alcohol yield surpasses the aromatics yield.

The detailed yields of the individual molecule in P27 over the four catalysts are plotted in Figures 2 (the alcohols) and 3 (the

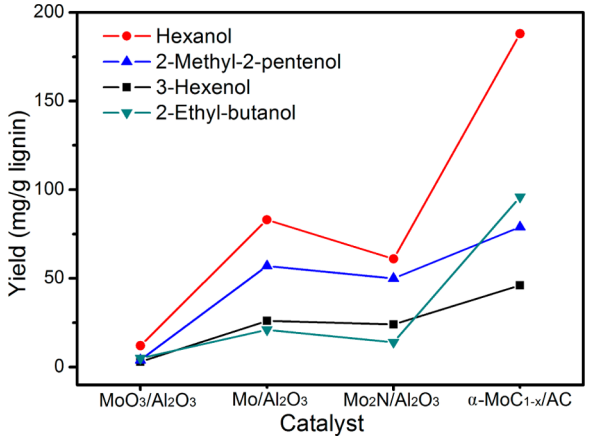

Figure 2. Detailed quantified yield of alcohols from the lignin catalytic valorization experiment. (Reaction conditions: 1.0 g of Kraft lignin, 0.5 g of catalyst, initial 0.1 MPa of N_2, 100 mL of ethanol, 553 K, 6 h.)

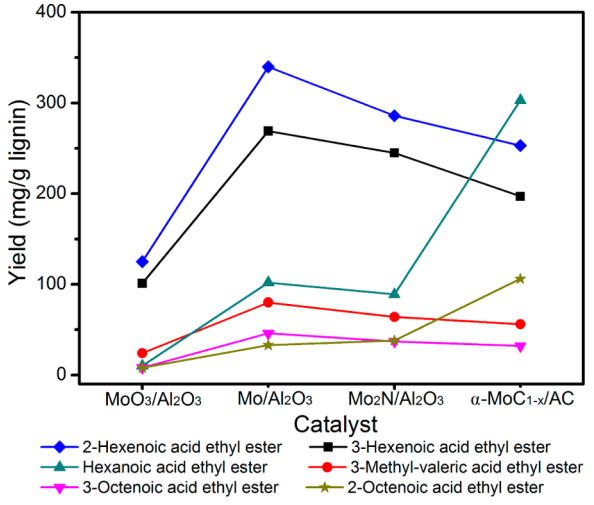

Figure 3. Detailed quantified esters yield from the lignin catalytic valorization experiment. (Reaction conditions: 1.0 g of Kraft lignin, 0.5 g of catalyst, initial 0.1 MPa of N_2, 100 mL of ethanol, 553 K, 6 h.)

esters) and listed in Table 1 (the aromatics). For the quantified alcohols, no matter which catalyst was used, hexanol accounts for the most, being as high as 188 mg/g of lignin over the carbide. The alcohols that followed were 2-methyl-2-pentenol, 3-hexenol, and 2-ethyl-butanol over the Mo/Al_2O_3 and Mo_2N/Al_2O_3 catalysts. Over α-MoC_{1-x}/AC, the sequence is 2-ethyl-butanol > 2-methy-2-pentenol > 3-hexenol. The highest overall yield of the alcohols was obtained over the α-MoC_{1-x}/AC catalyst, 409 mg/g of lignin, and the least was 24 mg/g of lignin over the MoO_3/Al_2O_3 catalyst. For the Mo/Al_2O_3 and Mo_2N/Al_2O_3 catalysts, the overall alcohol yields are 187 and 149 mg/g of lignin, respectively. The ester with the highest yield, 340 mg/g of lignin, achieved over Mo/Al_2O_3, is 2-hexenoic acid ethyl

DOI: 10.1021/acscatal.5b01159
ACS Catal. 2015, 5, 4803−4813

Table 1. Detailed Quantified Aromatic Products from the Lignin Catalytic Ethanolysis[a]

Entry	Catalyst	Benzyl alcohols					Monophenols					Arenes						
1	MoO_3/Al_2O_3	-	-	6	-	2	-	-	6	2	-	14	1	4	7	4	5	-
2	Mo/Al_2O_3	8	78	31	18	27	-	21	23	6	10	47	3	4	16	19	21	-
3	Mo_2N/Al_2O_3	24	71	31	7	21	3	15	0	6	7	34	2	5	12	15	17	6
4	α-MoC_{1-x}/AC	13	14	21	13	10	4	-	35	16	23	56	12	33	14	3	-	13

[a]Reaction conditions: 1.0 g of Kraft lignin, 0.5 g of catalyst, initial 0.1 MPa of N_2, 100 mL of ethanol, 553 K, 6 h. Notes: "-" means not detected.

Table 2. Summary of the Identified but Unquantified Products from the Lignin Catalytic Ethanolysis Reactions

Aliphatics	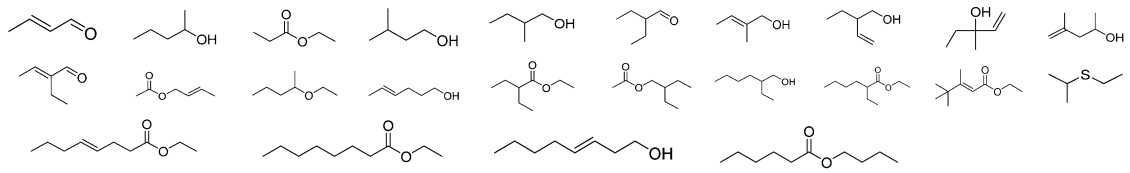
Aromatics	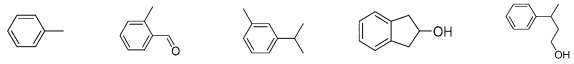

Table 3. Detailed Yields (mg/g of lignin) of the Products from Ethanol Self-Evolution Reactions without and with Lignin Added at 553 K for 6 h over 0.5 g Mo/Al_2O_3 Catalyst with Initial 0.1 MPa of N_2 and 100 mL of Ethanol

	Aliphatics										
Without KL	879	1615	917	2	7	651	80	25	21	26	30
With KL	566	526	982	410	3	79	58	60	17	3	4

ester (Figure 3). Hexanoic acid ethyl ester, 303 mg/g lignin, obtained over the α-MoC_{1-x}/AC catalyst followed.

The overall yield of esters with 10 carbons is much lower than that of the esters with eight carbons over all four catalysts. The highest overall ester yield was 947 mg/g of lignin, obtained over the α-MoC_{1-x}/AC catalyst, followed by 870, 759, and 276 mg/g of lignin over the Mo/Al_2O_3, Mo_2N/Al_2O_3, and MoO_3/Al_2O_3 catalysts, respectively. The aromatic compounds obtained in this work are mainly benzyl alcohols, monophenols, and arenes. Over the MoO_3/Al_2O_3 catalyst, the overall yield of aromatics was only 51 mg/g of lignin. The values were 332, 276, and 280 mg/g of lignin, respectively, for the Mo/Al_2O_3, Mo_2N/Al_2O_3, and α-MoC_{1-x}/AC catalysts. The highest benzyl alcohols yield, 162 mg/g of lignin, was obtained when Mo/Al_2O_3 was used, followed by 154 mg/g of lignin over the Mo_2N/Al_2O_3 catalyst and 71 mg/g of lignin over the α-MoC_{1-x}/AC catalyst.

On the α-MoC_{1-x}/AC catalyst, the highest overall yields of monophenols and arenes were obtained: 78 and 131 mg/g of lignin, respectively. The overall yields of monophenols and arenes were 60 and 110 mg/g of lignin, respectively, over the Mo/Al_2O_3 catalyst. The two values are 31 and 91 mg/g of lignin over the Mo_2N/Al_2O_3 catalyst. The other 29 identified products are listed in Table 2. Most of them are aliphatic compounds. In the GC/FID spectrum, although the yields for individual molecules are much lower than that of the least produced molecule in the P27, these 29 molecules account for 16% of the overall integrated peak area of the molecules produced, with the involvement of lignin in the case of α-MoC_{1-x}/AC as the catalyst.[26] The four Mo-containing catalysts presented here show extraordinary performance in the lignin conversion reaction in supercritical ethanol and give promising overall yields of high-valued C6−C10 oxygenated products without tar and char formation.

Table 3 lists the yields of 11 molecules, believed to be produced from the self-reactions of ethanol derived intermediates, without and with lignin in the reaction system over the Mo/Al_2O_3 catalyst. The formation of these products was also verified by heating ethanol and the α-MoC_{1-x}/AC catalyst together under the same conditions.[26] Without lignin in the reaction, acetaldehyde, ethyl acetate, butanol, and 1,1-diethoxyethane are the main products, with yields of 879, 1615, 917, and 651 mg/g of lignin, respectively. It is noted that, for the sake of easy comparison, the data are expressed as milligrams of product per 1 gram of lignin, even for the case without putting lignin here. This is sensible because the reaction volume is exactly the same, and the amount of lignin in the reactions with lignin is also the same. When lignin was added, the main products changed. Now, these are acetaldehyde, ethyl acetate, butanol, and 2-butenol, with yields of 566, 526, 982, and 410 mg/g of lignin, respectively.

Along with the great decrease in the yield of ethyl acetate, the yield of 1,1-diethoxyethane drops sharply from 651 to 79 mg/g of lignin. The yields of the other two acetals, both 1,1-diethoxybutane and 1-(1-ethoxyethoxy)-butane decrease, from 26 and 30 mg/g of lignin to 3 and 4 mg/g of lignin,

DOI: 10.1021/acscatal.5b01159
ACS Catal. 2015, 5, 4803−4813

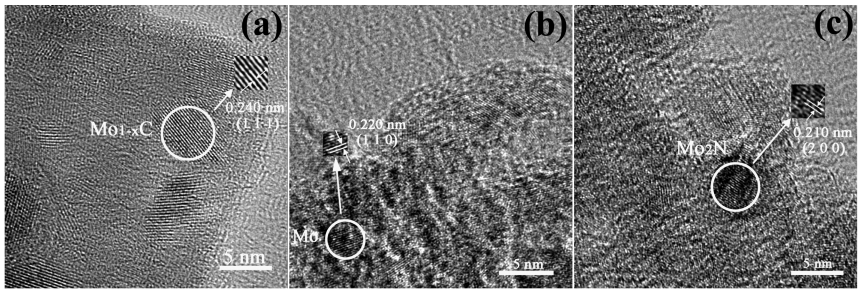

(d)

Sample	Specific surface area (m^2/g)	Total pore volume (cm^3/g)	Average pore diameter (nm)
α-MoC_{1-x}/AC	749	0.71	7.9
Mo/Al_2O_3	181	0.45	10.0
Mo_2N/Al_2O_3	169	0.46	10.9
MoO_3/Al_2O_3	118	0.31	10.6

Figure 4. Representative TEM images of the (a) α-MoC_{1-x}/AC, (b) Mo/Al_2O_3, (c) Mo_2N/Al_2O_3, and (d) textural properties of the catalysts.

respectively. The yields of butyric acid ethyl ester and 2-butenoic acid ethyl ester also decline from 80 and 21 to 58 and 17 mg/g of lignin, respectively. For acetic acid butyl ester, the yield increases from 25 to 60 mg/g of lignin, and this may be ascribed to the increased formation of butanol in the reaction system. No clear change in the yield of 1-ethoxy-1-butene was observed. These results indicate that the depolymerization of lignin fragments consumes the precursors of acetaldehyde, ethyl acetate, 1,1-diethoxyethane, 1-diethoxybutane, 1-(1-ethoxyethoxy)-butane, butyric acid ethyl ester, and 2-butenoic acid ethyl ester. However, the presence of lignin and its derivatives favor the formation of butanol, 2-butenol, and acetic acid butyl ester.

3.2. Catalyst Characterization. Figure 4 shows TEM images and surface area information on the catalysts. Compared with the alumina supported catalyst, the carbide catalyst possesses a larger specific surface area and total pore volume and a clearer crystal lattice. Figure 5 gives the XRD patterns of both the fresh and the used catalyst samples. All the fresh Mo-based catalysts display typical diffraction patterns in accordance with their phase compositions. The Mo metal, oxide, nitride, and carbide present their characteristic peaks in their patterns. The alumina support exhibits weak peaks at 2θ = 45.9 and 66.8°, whereas the activated carbon does not show any phase features in the diffraction pattern. After reaction, the major diffraction peaks of the samples are retained, but the peak intensities are weakened, and a few new peaks attributed to an oxide phase also appear. The stability of the Mo-based catalysts in the lignin decomposition reaction in supercritical ethanol is also verified by the reuse of the catalysts. After three cycles, the product yields decline to about ~80% of the initial yields for the nitride and carbide catalysts. The loss of activity can probably be related to partial leaching of the metal, as detected via ICP (data not shown), which is probably partly responsible for the loss of crystallinity, as well.

Here, the Mo-based catalysts, although with different phase structures and energetic states, all exhibit remarkable activity in the reaction, with the metallic, carbided, and nitrided samples performing at similarly high activities. A genuinely active species should exist. Figure 6 depicts the infrared spectra of the catalyst samples after the reaction. For the used Mo/Al_2O_3

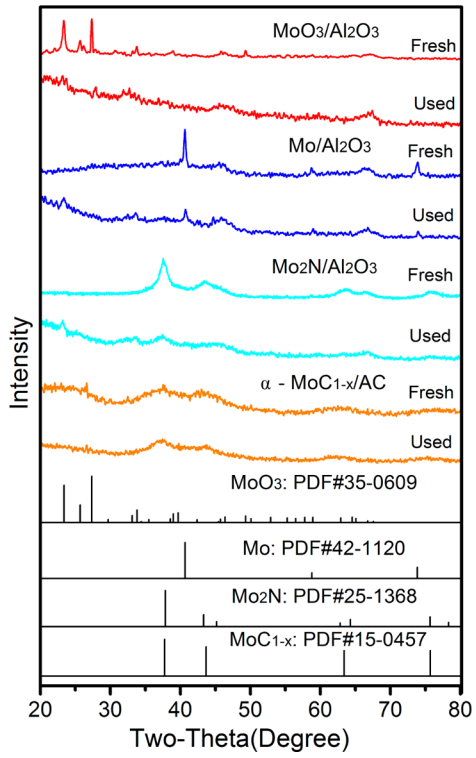

Figure 5. Powder XRD patterns of the catalysts before and after the reaction.

(curve b), α-MoC_{1-x}/AC (curve c), and Mo_2N/Al_2O_3 (curve d), a band at 622 cm^{-1} is clearly observed that is attributed to the Mo−O stretching vibration.[28−30] For the used MoO_3/Al_2O_3 (curve a), the broad band centered at around 600 cm^{-1} involves the Mo−O stretching vibration in which the O atom is linked to three molybdenum atoms, whereas the absorption at 882 cm^{-1} comes from the stretching vibration of Mo−O in which the O atom is linked to two molybdenum atoms in a Mo−O−Mo entity.[30−32] For the four catalysts, the absorption bands observed at the 1450 and 1380 cm^{-1}, attributed to the C−H bending vibrations, and the 1125 cm^{-1} band belonging to the C−O stretching vibrations, are plausibly attributed to the

DOI: 10.1021/acscatal.5b01159
ACS Catal. 2015, 5, 4803−4813

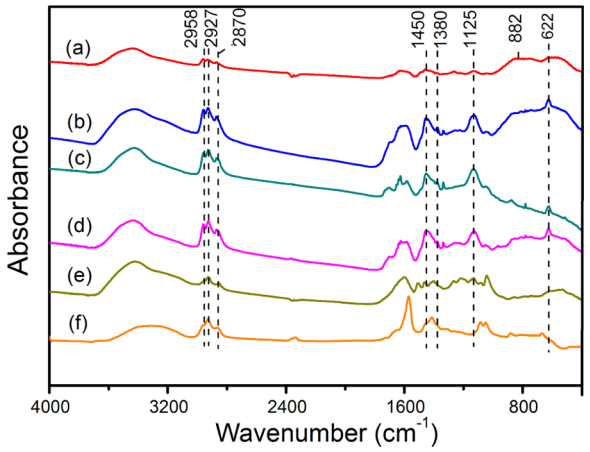

Figure 6. FT-IR spectra of the lignin, the product, and the used catalyst samples. (a) Used MoO_3/Al_2O_3, (b) used Mo/Al_2O_3, (c) used α-MoC_{1-x}/AC, (d) used Mo_2N/Al_2O_3, (e) Kraft lignin, and (f) dried liquid product from lignin catalyzed by Mo/Al_2O_3.

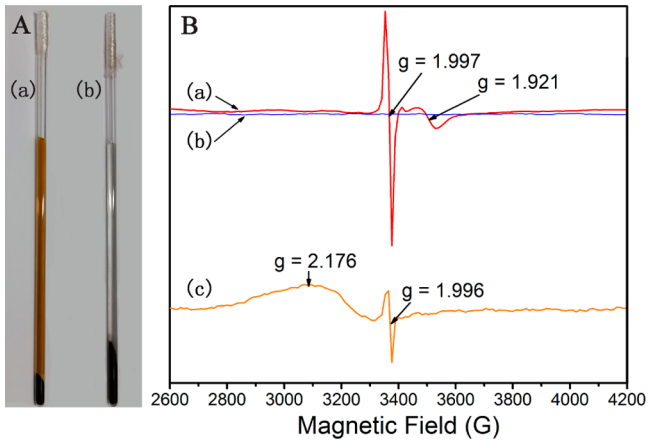

Figure 7. Photos and EPR curves of the used and fresh catalyst samples free of air contact. (A) Photographs of (a) used Mo/Al_2O_3 catalyst with liquid products and (b) fresh Mo/Al_2O_3 catalyst with ethanol in EPR sample cell. (B) EPR spectra of (a) used Mo/Al_2O_3 catalyst, (b) fresh Mo/Al_2O_3 catalyst, and (c) Kraft lignin.

adsorbed ethoxide.[33] Clarifying further, the spectra of the initial Kraft lignin (curve e) and the liquid product (curve f) after evaporation of the ethanol solvent are also presented. The bands at 2958, 2927, and 2870 cm^{-1}, which are due to the $-CH_3$ and $=CH_2$ stretching vibrations, are also observed in the spectra of the four used catalysts (curves a–d). For the alumina-supported samples, the strong IR absorption below 1000 cm^{-1} is due to the ionic characteristics of the Al–O bond in alumina.[34] The broad band around 3450 cm^{-1} is due to the stretching vibration of AlO–H bond and the vibration of HO–H of water molecules adsorbed on the surface, whereas the band at ~1600 cm^{-1} is due to the bending vibration of trapped water molecules.[35,36] On the basis of the above analysis, we conclude that all the molybdenum compound in the different catalysts, except MoO_3, was oxidized partially to a state with Mo–O bond (or Mo=O) during the reaction, and this was also reflected in the XRD patterns to a certain extent. This state may be related to the genuinely catalytically active species for the lignin conversion under supercritical ethanol conditions. In addition, the spectra of the used catalysts do not show the absorption peaks related to the Kraft lignin in the range from 1800 to 1000 cm^{-1}, indicating that the lignin is fully converted, which is in good agreement with our reported results.[26]

To explore further the change in the Mo valence state during the reaction, EPR spectra (Figure 7) of the used catalysts were collected. To eliminate the possible influence of air during filtration for separating the liquid products and the used catalyst, the sample including the liquid products, solvent, and the used Mo/Al_2O_3 catalyst was directly filled into the EPR cell, as shown in Figure 7A-a, with a capillary pipet after reaction to avoid contact with air. The spectra were recorded at liquid nitrogen temperature. The EPR spectra of three samples are illustrated in Figure 7B. A clear signal (curve a) owing to the presence of paramagnetic Mo(V) with g = 1.921 was observed in the EPR spectrum of the used Mo/Al_2O_3 sample.[37,38] We also did the EPR measurement of the fresh Mo/Al_2O_3 catalyst preserved in ethanol without any exposure to air after the preparation (Figure 7A-b). No Mo(V) signal was detected because of the nonexistence of the paramagnetic species (curve b). Therefore, we are quite sure that the molybdenum was partially oxidized during the reaction.

The EPR spectra of the other used Mo-based catalysts were also recorded, and the signal with a g tensor of about 1.92 was observed with all the samples. Che et al. suggested that Mo(V) has a short Mo=O bond and is surrounded only by oxygen ligands.[39,40] The intense signal at g = 1.997 is due to the free electrons of the condensed aromatics or the graphite-like coke.[38,41] In the Kraft lignin sample (curve c), a narrow signal of g = 1.996 was recorded, corresponding to the organic free radicals existing in the lignin.[42,43] The signal with a peak at g = 2.176 is possibly associated with the metal ions existing as ash in the lignin. In a previous report, adsorption of Mn (II) onto lignin extracted from wheat straw caused a plateau at g = 2.16.[42] Referring to the results of the FT-IR analysis, the partial oxidation of Mo at the surface of the active phase during the lignin conversion reaction is well proved; however, the bulk active Mo phases of the catalysts do not change much during the reaction, as elucidated with the data of the XRD analysis.

3.3. Proposal of a Scheme of the Reaction. Recently, Román-Leshkov's group demonstrated that MoO_3 is an active catalyst for the HDO of various biomass-derived oxygenates, including aliphatic and cyclic ketones, furanics, and phenol feeds. MoO_3 was proved to selectively cleave C–O bonds to produce olefinic and aromatic hydrocarbons with high activity and selectivity using low H_2 pressures (<1 bar) at 593 K.[44,45] In the reaction mechanism proposed, Mo^{5+} species generated either from the carburization of MoO_3 to $MoO_xC_yH_z$ or during the reduction of MoO_3 to MoO_{3-x} in the presence of H_2 were believed to be responsible for the HDO chemistry, and Mo^{4+} state species were completely inactive for the HDO of phenolic compounds, which was proved from the control experiments.[45]

In lignin conversion, as the insoluble solid lignin meets heterogeneous catalysts in ethanol, mass transfer becomes limited and may retard the catalytic reaction. Although several studies have reported heterogeneously catalyzed conversion of lignin, the mechanism is far less elucidated.[15] Moreover, no insight into the mechanism of lignin conversion to diverse chemicals over Mo-based catalysts has been reported. Here, in our reaction systems with Mo-based catalysts for lignin conversion, the metallic, carbided, and nitrided Mo all showed similarly high activities toward lignin depolymerization to C6–C10 molecules, although with different yields of the specific products, whereas in our previous work, with the aid of a

DOI: 10.1021/acscatal.5b01159
ACS Catal. 2015, 5, 4803–4813

Scheme 1. Possible Reaction Pathways of (a) Ethanolysis of Lignin and Formation of Active Mo Species and (b, c) Formation of the Final Products

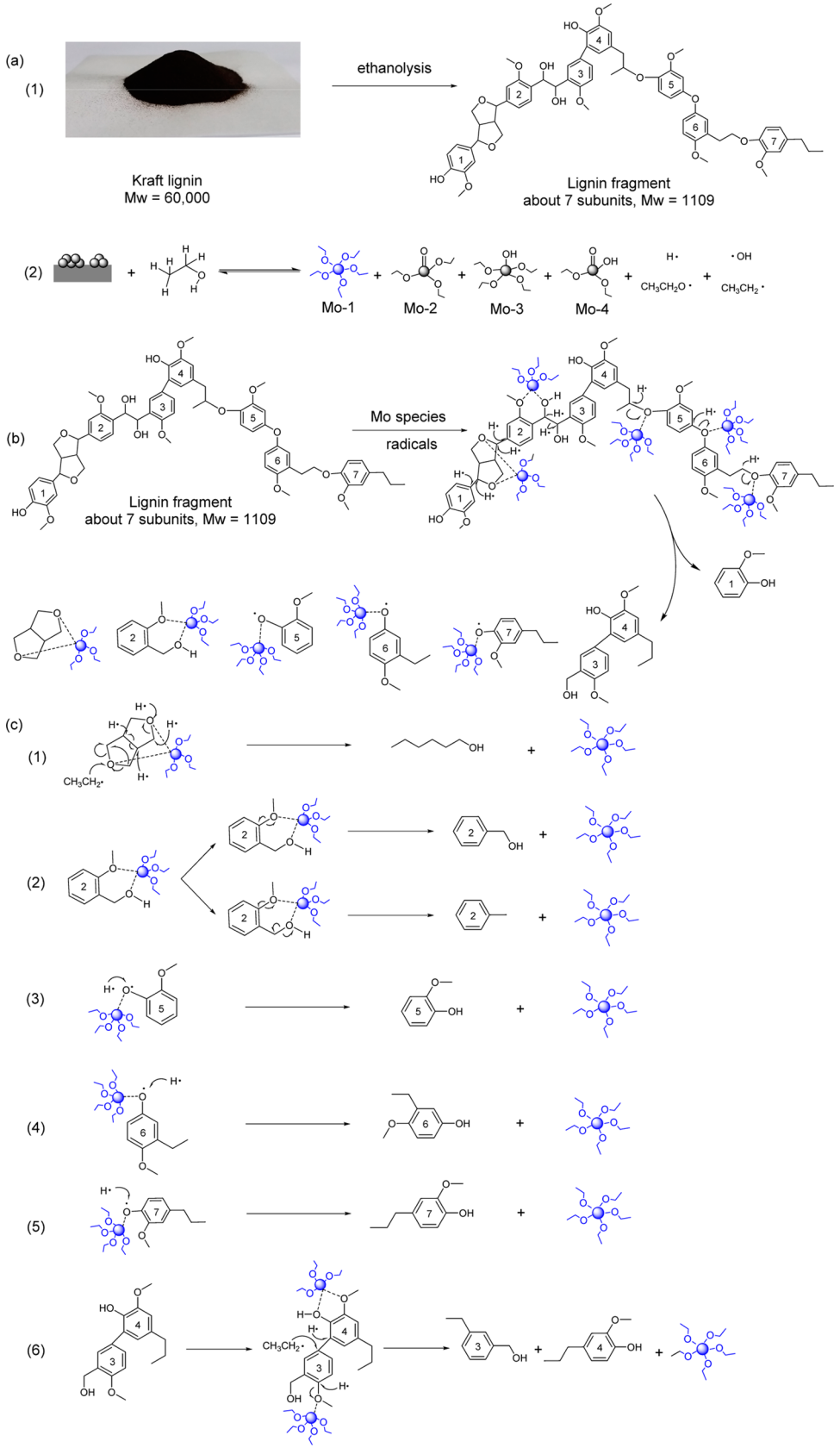

matrix-assisted laser desorption/ionization time-of-flight mass spectrometry (MALDI-TOFMS) technique, Kraft lignin was found to be degraded into fragments with molecular weights in a range of m/z of 700−1400 in supercritical ethanol without a

DOI: 10.1021/acscatal.5b01159
ACS Catal. 2015, 5, 4803−4813

Scheme 2. Reaction Pathways of the Related Ethanol Conversion. Production Route of (a) Acetaldehyde, (b) Ethyl Acetate and Acetal, (c) Butanol, (d) Butyric Acid Ethyl Ester and 1,1-Diethoxybutane, and (e) Acetic Acid Butyl Ester and 1-(1-Ethoxyethoxy)-butane

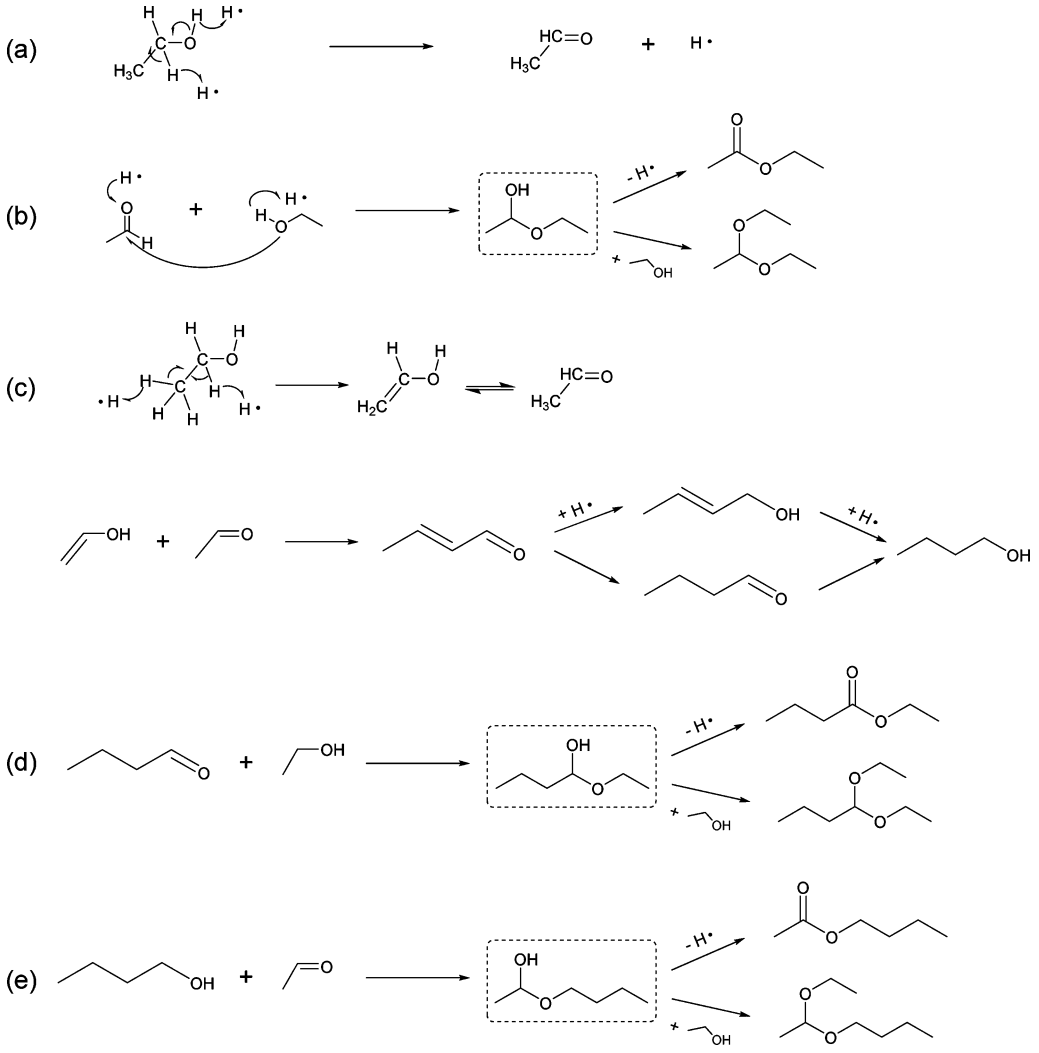

catalyst.[26] This is possible due to that the radicals generated from supercritical alcohol serve as the ethanolysis agent, depolymerizing the lignin into intermediate segments and stabilizing the segments via a capping effect of the hydrogen or ethoxy radicals.[46] Song et al. examined the valorization of birch wood lignin into monomeric phenols over nickel-based catalysts in different alcohols, including methanol, ethanol, and ethylene glycol, and proposed that lignin is first fragmented into smaller lignin intermediates with $m/z \sim 1100-1600$ via an alcoholysis pathway, then followed by the hydrogenolysis steps resulting in the production of phenols.[15]

On the basis of the above-reported results and our analysis, the preliminary reaction pathways of the Kraft lignin valorization in supercritical ethanol are proposed. The reaction steps mainly contain the noncatalytic ethanolysis of lignin into fragments and further catalytic conversion of the fragments to final small molecules with the interaction with the radicals generated from ethanol either on the surface of the Mo-based catalysts or on the detached Mo species in the fluid phase. Here, the first step is illustrated as Scheme 1a-1, giving a lignin segment with seven benzene rings and a molecular weight of 1109 g/mol. Meanwhile, at the catalyst surface, ethanolysis of the Mo−Mo, Mo−N, and Mo−C bonds happens and leads to the formation of the common active Mo species, as shown in Scheme 1a-2, that is, the partially and fully ethanolyzed Mo species, as marked in the scheme as Mo-1, Mo-2, Mo-3, and Mo-4. Some of the species enters the fluid phase, while some remain on the catalyst surface. Molybdenum ethoxide (Mo-1) is certainly formed, just like the soluble H_xWO_3 reported in the cellulose conversion in high temperature water.[47] In the oxidation of ethanol on molybdenum oxide catalysts, Mo−OC_2H_5 was supposed to be the intermediate.[48] In addition, molybdenum ethoxide ($Mo(OEt)_5$) was found to be an effective catalyst in the polymerization of acetylene and propargyl derivatives in early times.[49,50] We also test the activity of molybdenum ethoxide prepared according to a patent,[51] and the obtained total products (also consisting of similar alcohols, esters, and aromatics) yield from the lignin conversion reaction was 690 mg/g of lignin. This verifies the activity of the Mo-1 species.

In the pathways postulated hereafter, Mo-1 is taken as the main active species because it is easier to dissociate in the fluid phase compared with the others. The Mo-based catalyst also contributes to the formation of the diverse radicals from ethanol. Because of the rich presence of the dissociative Mo active species, radicals, and the lignin segments, the mass

DOI: 10.1021/acscatal.5b01159
ACS Catal. 2015, 5, 4803−4813

Scheme 3. Reaction Pathways of the Products Formation with Different Radical Stabilization and Interactions[a]

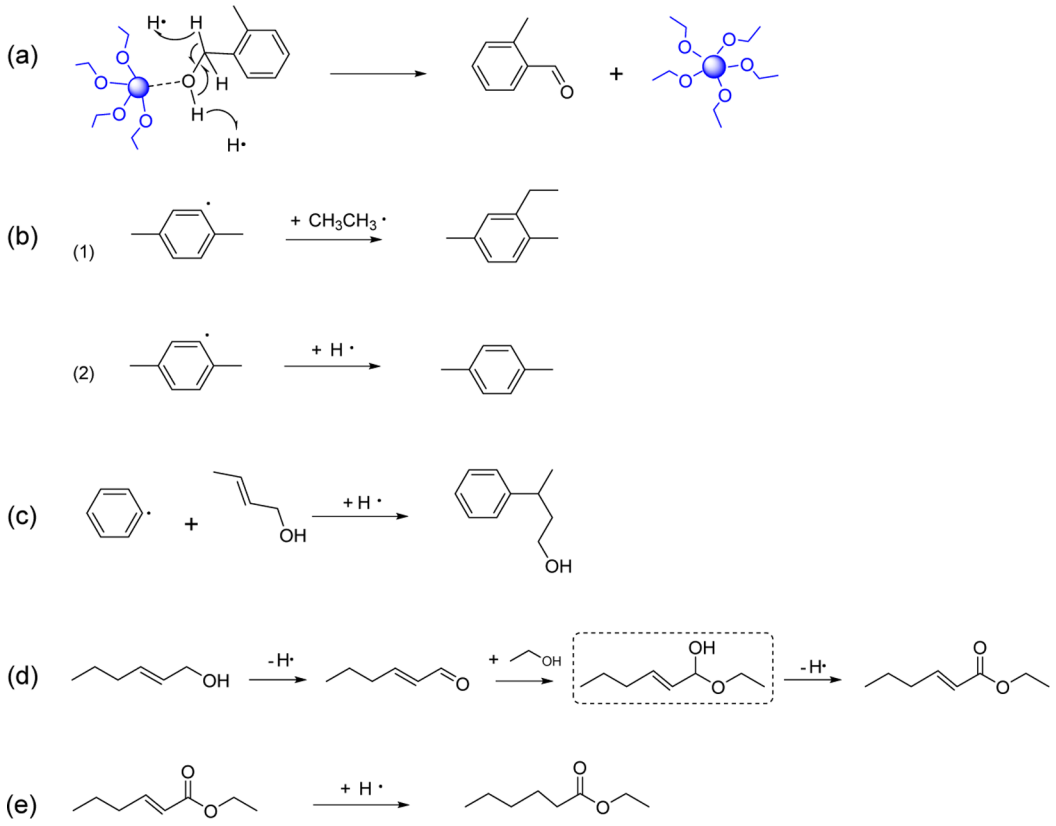

[a](a–c) Stabilization of active aromatic radicals, (d, e) stabilization of related aliphatic alcohols and esters in the reaction system.

transfer and the geometrical limitations between the solid catalyst and the reactant are eliminated. As shown in Scheme 1b, the Mo species then attack the lignin segments or molecules originating from with medium molecular weight through forming coordination bonds between the lone electron pairs of the oxygen atoms and the unoccupied d orbitals of the Mo ions. Hence, the segments are further decomposed. As a consequence, the formed active intermediates and the small molecules with active functional groups are stabilized by the rich radicals such as hydrogen, ethyl, and ethoxyl. Thus, the diverse compounds, including benzyl alcohols, phenols, and arenes, are produced. Guaiacol (numbered 1) is directly produced from the segment disruption. Hexanol is more likely generated from the interaction of the radicals and the lignin aliphatic segment on the active site (Scheme 1c-1). Number 2 species fractions on the Mo-1 site and directly forms benzyl alcohol; however, the C−O ether bond can also be cleaved and can form an active phenyl group, then because of the interaction with the active hydrogen, the phenyl group turns to toluene (Scheme 1c-2).

o-Methyl benzyl alcohol is the main product in the quantified five benzyl alcohols over the Mo/Al_2O_3 and Mo_2N/Al_2O_3 catalysts, whereas over α-MoC_{1-x}/AC catalyst, *o*-methyl benzyl alcohol and *p*-methyl benzyl alcohol are the main products. o-Xylene is the main arene product over all the four molybdenum-based catalysts. Guaiacol is derived from the numbered 5 portion on the Mo site (Scheme 1c-3), and alkyl-guaiacol can directly form from the fragment (Scheme 1c-4,5). Alkylation reactions also happen on guaiacol and lead to the other phenols in the product, such as methyl guaiacol, ethyl guaiacol and propyl guaiacol.[19] For the small segments with pieces numbered 3 and 4, the benzene rings are attacked by the active hydrogen and ethyl radicals on the surface of the active site and finally result in *m*-ethyl benzyl alcohol and *p*-propyl guaiacol formation simultaneously (Scheme 1c-6).

Without lignin, but with ethanol and supported metallic molybdenum catalyst in the reactor, 11 kinds of aliphatic compounds, mainly ethyl acetate, butanol, and acetal, were detected under the same reaction conditions. These products or their precursors contribute greatly to the formationof the final products, especially the aliphatic alcohols and esters. Scheme 2 refines the routes of the formation of aliphatic compounds from ethanol. Acetaldehyde is first produced from the dehydrogenation of ethanol.[48,52] Following that, hemiacetal is formed from the reaction between ethanol and acetaldehyde (Scheme 2b). Hemiacetal acts as an intermediate, verified by its absence in the GC/MS spectrum after 6 h of reaction with lignin. After dehydrogenation of hemiacetal, ethyl acetate is formed, and acetal is produced through the reaction between hemiacetal and ethanol.[52] With the addition of lignin, large decreases in ethyl acetate and acetal yields are related to the decrease in the acetaldehyde in the system and the enhanced consumption of the radicals formed from ethanol self-revolution reactions.

Butanol production from ethanol has been widely reported.[53−56] The process consists of mainly dehydrogenation and keto−enol tautomerism of acetaldehyde, aldol condensation, and hydrogenation steps[54] (Scheme 2c). During the aldol condensation and the following hydrogenation, butanal, butenal, and butenol are also produced. Through the interactions between ethanol and butanal on the active site, 1,1-diethoxybutane and butyric acid ethyl ester are formed

DOI: 10.1021/acscatal.5b01159
ACS Catal. 2015, 5, 4803−4813

(Scheme 2d). Acetaldehyde can also react with butanol, thus leading to the formation of acetic acid butyl ester and 1-(1-ethoxyethoxy)-butane (Scheme 2e). Most of the small molecules formed in the steps outlined in Scheme 2 can further react with and stabilize the radicals formed from the lignin fragmentation, thus preventing the condensation of the intermediates (Scheme 3). In the reported results in the literature, ethanol has also been assumed to react via alkylation and esterification reactions with lignin fragments.[19] Furthermore, the mutual transformation and alkylation reactions among the intermediate products, from not only ethanol but also from lignin, contribute to the diversity of the final products.

Several esters, for example, hexanoic acid ethyl ester, 2-hexenoic acid ethyl ester, 3-hexenoic acid ethyl ester and 3-methyl valeric acid ethyl ester, are believed to have relationship with the carbohydrate linkages or hexenuronic acid groups in the lignin pieces, which are likely formed during the Kraft pulping process.[7,57] Nevertheless, the Guerbet reaction, often used to increase the carbon number of alcohols, contributes to the formation of higher alcohols.[19,26,55] Octenol was detected in the products, although at small amount. The interaction between octenol and ethanol results in the formation of octenoic acid ethyl esters and octanoic acid ethyl ester. Because the active sites are derived from the catalyst with different Mo-based phases, the kind and amount of the dissociative Mo species are different in the reaction system, which in turn leads to the difference in the product distribution for the different catalysts. The difference in the yield of a specific product over different catalysts also depends on the comparative ability of the catalyst in generating the different active species listed in Scheme 1a-2. In addition, although the Mo/Al_2O_3 catalyst gives slightly lower yields when compared with the carbide catalyst (according to Figure 1), its use can be justified on the basis of the simplicity and cost of production.

4. CONCLUSIONS

In summary, we have proposed the reaction pathways of Kraft lignin valorization into high-valued chemicals over molybdenum-based catalysts in supercritical ethanol. Lignin was converted to diverse products mainly containing aliphatic alcohols, esters, monophenols, benzyl alcohols, and arenes. Four Mo-based catalysts showed activities with an activity sequence of carbide > metal > nitride > oxide. The total product yields are 1636, 1390, 1185, and 351 mg/g of lignin, respectively for the four catalysts. Metallic Mo gives the highest overall aromatic product yield, 333 mg/g of lignin, and the carbide produces the highest esters yield of 947 mg/g of lignin. Supercritical ethanol not only acts as an inert solvent but also participates in the reaction, thus resulting in an overall product yield exceeding 100 wt %.

Combined with the XRD and FT-IR analysis, Mo was proved to be partially oxidized (except MoO_3), although the bulk structures of the active phases in the catalysts were well preserved after the reaction. EPR spectra further proved the presence of Mo(V) species. The preliminary reaction pathways of the lignin decomposition over the Mo-based catalysts in supercritical ethanol are proposed. Lignin experiences a noncatalytic ethanolysis step and forms intermediate segments with a molecular weight of $m/z \sim 700-1400$. After that, the dissociative Mo active species, especially with high ethoxyl content facilitates the complete decomposition of the segments. Meanwhile, the diverse radicals from ethanol and ethanol-derived compounds also participate in the reaction, playing important roles in stabilizing and suppressing the condensation of the original products. Finally, the diverse value-added small oxygenated and aromatic molecules are formed.

AUTHOR INFORMATION

Corresponding Author

*Phone: +86-22-27405613. Fax: +86-22-27405243. E-mail: ydli@tju.edu.cn.

Author Contributions

†X.M. and R.M. contributed equally to this work.

Notes

The authors declare no competing financial interest.

ACKNOWLEDGMENTS

The financial support from the Ministry of Science and Technology of China under Contract No. 2011DFA41000 and the Natural Science Foundation of China under Contract No. 21336008 are gratefully acknowledged. This research was also supported in part by the Program of Introducing Talents to the University Disciplines under File No. B06006 and the Program for Changjiang Scholars and Innovative Research Teams in Universities under File No. IRT 0641. The authors thank Professor Julian R. H. Ross of the University of Limerick and Professor Paul Dyson for their invaluable discussions.

REFERENCES

(1) Chu, S.; Majumdar, A. *Nature* **2012**, *488*, 294−303.
(2) Shui, H.; Shan, C.; Cai, Z.; Wang, Z.; Lei, Z.; Ren, S.; Pan, C.; Li, H. *Energy* **2011**, *36*, 6645−6650.
(3) Tong, X. L.; Ma, Y.; Li, Y. D. *Appl. Catal., A* **2010**, *385*, 1−13.
(4) Berl, E. *Science* **1944**, *99*, 309−312.
(5) Ragauskas, A. J.; Beckham, G. T.; Biddy, M. J.; Chandra, R.; Chen, F.; Davis, M. F.; Davison, B. H.; Dixon, R. A.; Gilna, P.; Keller, M.; Langan, P.; Naskar, A. K.; Saddler, J. N.; Tschaplinski, T. J.; Tuskan, G. A.; Wyman, C. E. *Science* **2014**, *344*, 1246843.
(6) Huber, G. W.; Iborra, S.; Corma, A. *Chem. Rev.* **2006**, *106*, 4044−4098.
(7) Zakzeski, J.; Bruijnincx, P. C. A.; Jongerius, A. L.; Weckhuysen, B. M. *Chem. Rev.* **2010**, *110*, 3552−3599.
(8) Freudenberg, K. *Science* **1965**, *148*, 595−600.
(9) Mahmood, N.; Yuan, Z.; Schmidt, J.; Xu, C. *Bioresour. Technol.* **2013**, *139*, 13−20.
(10) Yaman, S. *Energy Convers. Manage.* **2004**, *45*, 651−671.
(11) Peterson, A. A.; Vogel, F.; Lachance, R. P.; Fröling, M.; Antal, M. J., Jr; Tester, J. W. *Energy Environ. Sci.* **2008**, *1*, 32−65.
(12) Demirbas, A. *Energy Convers. Manage.* **2001**, *42*, 1357−1378.
(13) Ma, X.; Tian, Y.; Hao, W.; Ma, R.; Li, Y. D. *Appl. Catal., A* **2014**, *481*, 64−70.
(14) Zakzeski, J.; Jongerius, A. L.; Bruijnincx, P. C. A.; Weckhuysen, B. M. *ChemSusChem* **2012**, *5*, 1602−1609.
(15) Song, Q.; Wang, F.; Cai, J.; Wang, Y.; Zhang, J.; Yu, W.; Xu, J. *Energy Environ. Sci.* **2013**, *6*, 994−1007.
(16) Yan, N.; Zhao, C.; Dyson, P. J.; Wang, C.; Liu, L.; Kou, Y. *ChemSusChem* **2008**, *1*, 626−629.
(17) Jongerius, A. L.; Bruijnincx, P. C. A.; Weckhuysen, B. M. *Green Chem.* **2013**, *15*, 3049−3056.
(18) Matson, T. D.; Barta, K.; Iretskii, A. V.; Ford, P. C. *J. Am. Chem. Soc.* **2011**, *133*, 14090−14097.
(19) Huang, X.; Korányi, T. I.; Boot, M. D.; Hensen, E. J. M. *ChemSusChem* **2014**, *7*, 2276−2288.
(20) Deepa, A. K.; Dhepe, P. L. *ACS Catal.* **2015**, *5*, 365−379.
(21) Singh, S. K.; Ekhe, J. D. *RSC Adv.* **2014**, *4*, 27971−27978.
(22) Song, Q.; Wang, F.; Xu, J. *Chem. Commun.* **2012**, *48*, 7019−7021.

DOI: 10.1021/acscatal.5b01159
ACS Catal. 2015, 5, 4803−4813

(23) Grilc, M.; Likozar, B.; Levec, J. *Appl. Catal., B* **2014**, *150−151*, 275−287.
(24) Grilc, M.; Veryasov, G.; Likozar, B.; Jesih, A.; Levec, J. *Appl. Catal., B* **2015**, *163*, 467−477.
(25) Veryasov, G.; Grilc, M.; Likozar, B.; Jesih, A. *Catal. Commun.* **2014**, *46*, 183−186.
(26) Ma, R.; Hao, W.; Ma, X.; Tian, Y.; Li, Y. D. *Angew. Chem., Int. Ed.* **2014**, *53*, 7310−7315.
(27) Ma, X.; Cui, K.; Hao, W.; Ma, R.; Tian, Y.; Li, Y. D. *Bioresour. Technol.* **2015**, *192*, 17−22.
(28) Chisholm, M. H.; Reichert, W. W.; Thornton, P. *J. Am. Chem. Soc.* **1978**, *100*, 2744−2748.
(29) Seisenbaeva, G. A.; Kloo, L.; Werndrup, P.; Kessler, V. G. *Inorg. Chem.* **2001**, *40*, 3815−3818.
(30) El Shafei, G. M. S.; M. Mokhtar, M. *Colloids Surf., A* **1995**, *94*, 267−277.
(31) Seguin, L.; Figlarz, M.; Cavagnat, R.; Lassègues, J. C. *Spectrochim. Acta, Part A* **1995**, *51*, 1323−1344.
(32) Seyedmonir, S. R.; Howet, R. F. *J. Catal.* **1988**, *110*, 216−228.
(33) Medeiros, P. R. S.; Eon, J. G.; Appel, L. G. *Catal. Lett.* **2000**, *69*, 79−82.
(34) Wachs, I. E. *Catal. Today* **1996**, *27*, 437−455.
(35) Adam, F.; Iqbal, A. *Microporous Mesoporous Mater.* **2011**, *141*, 119−127.
(36) Knözinger, H.; Ratnasamy, P. *Catal. Rev.: Sci. Eng.* **1978**, *17*, 31−70.
(37) Brandhorst, M.; Cristol, S.; Capron, M.; Dujardin, C.; Vezin, H.; Le bourdon, G.; Payen, E. *Catal. Today* **2006**, *113*, 34−39.
(38) Liu, H.; Bao, X.; Xu, Y. *J. Catal.* **2006**, *239*, 441−450.
(39) Che, M.; McAteer, J. C.; Tench, A. J. *J. Chem. Soc., Faraday Trans. 1* **1978**, *74*, 2378−2384.
(40) Che, M.; Fournier, M.; Launay, J. P. *J. Chem. Phys.* **1979**, *71*, 1954−1960.
(41) Lange, J. P.; Gutsze, A.; Karge, H. G. *J. Catal.* **1988**, *114*, 136−143.
(42) Merdy, P.; Guillon, E.; Aplincourt, M. *New J. Chem.* **2002**, *26*, 1638−1645.
(43) Nakbanpote, W.; Goodman, B. A.; Thiravetyan, P. *Colloids Surf., A* **2007**, *304*, 7−13.
(44) Prasomsri, T.; Nimmanwudipong, T.; Román-Leshkov, Y. *Energy Environ. Sci.* **2013**, *6*, 1732−1738.
(45) Prasomsri, T.; Shetty, M.; Murugappan, K.; Román-Leshkov, Y. *Energy Environ. Sci.* **2014**, *7*, 2660−2669.
(46) Brand, S.; Susanti, R. F.; Kim, S. K.; Lee, H.; Kim, J.; Sang, B. *Energy* **2013**, *59*, 173−182.
(47) Wang, A.; Zhang, T. *Acc. Chem. Res.* **2013**, *46*, 1377−1386.
(48) Iwasawa, Y. *Acc. Chem. Res.* **1997**, *30*, 103−109.
(49) Gal, Y. S.; Jung, B.; Lee, W. C.; Choi, S. K. *Polymer (Korea)* **1992**, *16*, 597−603.
(50) Gal, Y. S.; Jung, B.; Cho, H. N.; Lee, W. C.; Choi, S. K. *Bull. Korean Chem. Soc.* **1992**, *13*, 4−5.
(51) Balthis, J. H., Jr.; Mendenhall, P.; Gresham, W. F.; Merckling, N. G. Du Pont, Wilmington, DE; Polymerization catalyst; U.S. Patent 3,038,863 A, June 12, 1962.
(52) Nishiguchi, T.; Matsumoto, T.; Kanai, H.; Utani, K.; Matsumura, Y.; Shen, W. J.; Imamura, S. *Appl. Catal., A* **2005**, *279*, 273−277.
(53) Scalbert, J.; Thibault-Starzyk, F.; Jacquot, R.; Morvan, D.; Meunier, F. *J. Catal.* **2014**, *311*, 28−32.
(54) Ogo, S.; Onda, A.; Iwasa, Y.; Hara, K.; Fukuoka, A.; Yanagisawa, K. *J. Catal.* **2012**, *296*, 24−30.
(55) Ndou, A. S.; Plint, N.; Coville, N. J. *Appl. Catal., A* **2003**, *251*, 337−345.
(56) Ogo, S.; Onda, A.; Yanagisawa, K. *Appl. Catal., A* **2011**, *402*, 188−195.
(57) Teleman, A.; Harjunpää, V.; Tenkanen, M.; Buchert, J.; Hausalo, T.; Drakenberg, T.; Vuorinen, T. *Carbohydr. Res.* **1995**, *272*, 55−71.

DOI: 10.1021/acscatal.5b01159
ACS Catal. 2015, 5, 4803−4813